Applied Mathematics & Information Sciences
An International Journal

A Complex-valued Solution of Free Vibration for Tapered Beams with Any Number of Rotational Dampers

Yong Chen[1] and Pan Liu[2]
[1]*College of Civil Engineering and Architecture, Zhejiang University, Hangzhou 310058, China*
[2]*Hangzhou Architectural Design and Research Institute Co., Ltd, Hangzhou 310001, China*
Email: cecheny@zju.edu.cn

Received: 11 Feb. 2012; Revised 16 May 2012; Accepted 01 Jul. 2012

Abstract: Exact analytical solution of free vibration for a linearly tapered beam with multiple arbitrarily placed rotational dampers is developed by taking advantage of the numerical assembly method (NAM) and Bessel functions. A characteristic equation for a tapered beam with any number of rotational dampers is therefore addressed in complex domain. Corresponding results for beams with different boundary conditions are also presented. The presence of the rotational dampers renders the solution of the characteristic equation complex valued. Therefore, a method is proposed to solve the equation in complex domain. To ensure the reliability of this method, the finite elements method (FEM) is used to verify the results achieved via the characteristic equation. Furthermore, with consideration of a single-rotational-damper case, the curves of the total maximum damping ratios and total optimal damping coefficients varying with taper ratios are also depicted for convenience of engineering application.

Keywords: Exact analytical solution, rotational damper, tapered beam, natural frequency, damping ratio.

1. Introduction

Using multiple dampers is benefit for simultaneously mitigating the vibrations of multiple modes. Free vibration of non-uniform beams has attracted many attentions. However, the study on the exact solutions of tapered beams with rotational dampers is rare. Thus, we are concerned with the exact analytical solution of transverse free vibration of a tapered beam attached with multiple rotational dampers.

Besides the approximate approaches, many exact analytical results were obtained by using Bessel functions to address the free vibrations of linearly tapered beams those without attachments [1-7]. For a tapered beam with attachments (such as point masses, linear springs and/or rotational springs),who leads to real-valued eigenvalues, the free-vibration-based study has attracted many attentions [8-14].

In literature, to the best knowledge of authors of this article, there is no investigation on the vibration of a tapered beam with rotational damper which renders the eigenvalues of the system complex valued. A few studies on the vibration of a uniform beam with rotational dampers were conducted. Oliveto et al. presented an exact solution of the free vibration of a simply supported beam with two rotational dampers attached at each end [15]. Krenk presented complex mode analysis on this problem [16]. By solving the root locus of the transfer functions, Engelen et al. derived the complex eigenvalues of a flexible structure including a viscous damper in terms of the mass and stiffness matrix equation of motion, and derived the formulas for the maximum damping ratio and the optimal damping constant [17]. Impollonia et al. conducted an analytical study on the dynamic characterization of a taut-cable with viscous rotational dampers and springs applied at the two ends [18]. Consider a problem of a tall building with damped outriggers, Chen et al. developed a simplified model consisting of a uniform beam and an arbitrary placed rotational damper, and provided an exact analytical solution of the problem and an approximate estimation of the system's modal damping ratios [19].

In this paper, the exact analytical solution for a tapered beam with multiple rotational dampers is studied. The motion equation for a tapered beam with multiple arbitrarily placed rotational dampers is set up based on D'Alembert's principle. Then, the non-dimensional characteristic equation of the beam-damper system could be obtained in terms of the idea of the numerical assembly method (NAM) which divides the beam into segments and treats the force of rotational dampers as boundary conditions.

Corresponding characteristic equation is suitable for a tapered beam with multiple rotational dampers and arbitrary manageable boundary conditions at ends. The method to solve this complex equation is proposed. Finite elements analysis FEA is used to verify the complex-valued results obtained by characteristic equation. As a non-proportional damping system, it is evident that there exists an optimal damping and maximum damping ratio in the system. With consideration of a single-rotational-damper case, natural frequencies and damping ratios for first five modes are attained, and curves for total maximum damping ratio and total optimal damping coefficient varying with taper ratios are also provided.

2. Problem formulations

As shown in Fig. 2.1, the non-uniform beam is attached with N rotational dampers sequentially. With consideration of an Euler-Bernoulli beam, the differential equation of a non-uniform beam is given by

$$\frac{\partial^2}{\partial x^2}\left[EI(x)\frac{\partial^2 y(x,t)}{\partial x^2}\right]+\rho A(x)\frac{\partial^2 y(x,t)}{\partial t^2}=0 \tag{1}$$

where $y(x,t)$ is the transverse displacement, E is Young's modulus, ρ is the mass density of the beam material, L is the span of the beam, and t is the time. Also, $A(x)$ is the cross-sectional area at the position x, $I(x)$ is the cross-sectional inertia, and they can be given by

$$A(x)=A_0\left[(\alpha-1)\frac{x}{L}+1\right]\left[(\beta-1)\frac{x}{L}+1\right] \tag{2a}$$

$$I(x)=I_0\left[(\alpha-1)\frac{x}{L}+1\right]\left[(\beta-1)\frac{x}{L}+1\right]^3 \tag{2b}$$

where $\alpha=b_1/b_0$ and $\beta=h_1/h_0$ are the taper ratios of the beam, A_0 and I_0 are the cross-sectional area and inertia at x=0 respectively, h_0 and h_1 are the cross-section heights at x=0 and x=L respectively, b_0 and b_1 are the cross-section widths at x=0 and x=L respectively.

The solution of Equation (1) can be expressed as

$$y(x,t)=Y(x)e^{i\omega t},\quad i=\sqrt{-1} \tag{3}$$

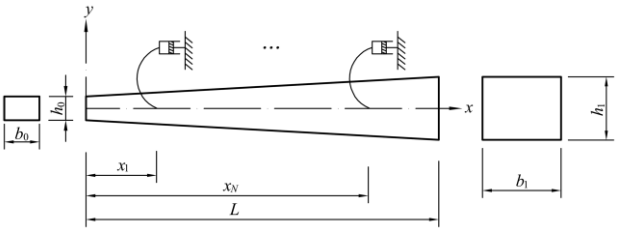

Figure. 2.1. A non-uniform beam with N rotational dampers.

By substitution of Equation (2) and Equation (3) into Equation (1), it yields

$$\begin{aligned}&\left[(\alpha-1)\frac{x}{L}+1\right]\left[(\beta-1)\frac{x}{L}+1\right]^3\frac{d^4Y(x)}{dx^4}+\\&2\left[(\beta-1)\frac{x}{L}+1\right]^2\left\{\left[(\beta-1)\frac{x}{L}+1\right]\frac{\alpha-1}{L}\right.\\&\left.+3\left[(\alpha-1)\frac{x}{L}+1\right]\right\}\frac{\beta-1}{L}\frac{d^3Y(x)}{dx^3}\\&+6\left[(\beta-1)\frac{x}{L}+1\right]\frac{\beta-1}{L}\left\{\left[(\beta-1)\frac{x}{L}+1\right]\frac{\alpha-1}{L}\right.\\&\left.+\left[(\alpha-1)\frac{x}{L}+1\right]\right\}\frac{\beta-1}{L}\frac{d^2Y(x)}{dx^2}\\&-\frac{\rho A_0\left[(\alpha-1)\frac{x}{L}+1\right]\left[(\beta-1)\frac{x}{L}+1\right]\omega^2}{EI_0}Y(x)=0\end{aligned} \tag{4}$$

In this paper, we consider merely that the taper ratios α and β are equal. Define the non-dimensional parameter

$$\gamma=\left[(\alpha-1)\frac{x}{L}+1\right]=\left[(\beta-1)\frac{x}{L}+1\right] \tag{5}$$

and

$$\tilde{x}=\frac{x}{L},\quad \tilde{Y}(\tilde{x})=\frac{Y(x)}{L} \tag{6}$$

Thus, Equation (4) yields

$$\gamma^4\tilde{Y}''''(\gamma)+8\gamma^3\tilde{Y}'''(\gamma)+12\gamma^2\tilde{Y}''(\gamma)-\frac{1}{16}\gamma^2\lambda^4\tilde{Y}(\gamma)=0 \tag{7}$$

where

$$\lambda^4=16\tilde{\omega}^2/(\alpha-1)^4 \tag{8}$$

where non-dimensional $\tilde{\omega}$ refers to the natural-frequency-related eigenvalue, and is defined as

$$\tilde{\omega}=\omega\left(L^2/h_0\right)\left(12\rho/E\right)^{1/2} \tag{9}$$

The general solution of Equation (7) can be written as

$$\tilde{Y}(\gamma)=\gamma^{-1}\left[T_1J_2\left(\lambda\sqrt{\gamma}\right)+T_2Y_2\left(\lambda\sqrt{\gamma}\right)+T_3I_2\left(\lambda\sqrt{\gamma}\right)+T_4K_2\left(\lambda\sqrt{\gamma}\right)\right] \tag{10}$$

and $T_j(j=1,\cdots,4)$ are the integration constants, J_2 and Y_2 are the second order Bessel function of first and second kinds. Also, I_2 and K_2 are the second order modified Bessel function of first and second kinds.

Equation (10) represents the eigenfunction of the transverse displacement of the beam. By disconnecting the beam at every rotational damper, the whole beam could be divided into $(N+1)$ segments. Free vibration of each segment has a form of Equation (10). The forces provided by rotational dampers can be therefore treated as boundary conditions. So the boundary conditions of the segments comprise displacement boundary conditions of the two ends, continuous conditions and force equilibrium conditions at the attaching point. By applying appropriate boundary conditions, and taking advantage of matrix, one can obtain the following coefficient equation for the beam system

$$\mathbf{DT}=0 \tag{11}$$

For a tapered beam attached with N rotational dampers, the coefficient vector **T** can be expressed as

$$\mathbf{T}=\left\{\mathbf{T}_1,\cdots,\mathbf{T}_n,\cdots,\mathbf{T}_{N+1}\right\}^{\mathrm{T}} \tag{12}$$

where $\mathbf{T}_n=\left\{T_{n1},T_{n2},T_{n3},T_{n4}\right\}^{\mathrm{T}}(n=1,2,\cdots,N+1)$, n is the sequential number of the segment, and $T_{nj}(j=1,\cdots,4)$ is the integration constants for the nth segment beam. The overall coefficient matrix **D** in Equation (11) can be expressed as

$$\mathbf{D}=\begin{bmatrix}\mathbf{D}_{\mathrm{L}} & \mathbf{0} & \mathbf{0} & \cdots & \mathbf{0} & \mathbf{0}\\ \mathbf{D}_{11} & \mathbf{D}_{12} & \mathbf{0} & \cdots & \mathbf{0} & \mathbf{0}\\ \mathbf{0} & \mathbf{D}_{21} & \mathbf{D}_{22} & \cdots & \mathbf{0} & \mathbf{0}\\ \vdots & \vdots & \ddots & \ddots & \vdots & \vdots\\ \mathbf{0} & \mathbf{0} & \mathbf{0} & \cdots & \mathbf{D}_{N1} & \mathbf{D}_{N2}\\ \mathbf{0} & \mathbf{0} & \mathbf{0} & \cdots & \mathbf{0} & \mathbf{D}_{\mathrm{R}}\end{bmatrix} \tag{13}$$

where **0** is a null matrix, $\mathbf{D}_{n1}$ and $\mathbf{D}_{n2}(n=1,2,\cdots,N)$ are 4×4 coefficient sub-matrixes those would be attained by applying the continuous conditions and force equilibrium conditions at the *n*th damper's location, $\mathbf{D}_{\mathrm{L}}$ and $\mathbf{D}_{\mathrm{R}}$ are 2×4 coefficient sub-matrixes those would be attained by applying the boundary conditions of the left and right ends respectively. These sub-matrixes of the overall coefficient matrix would be determined from the followings.

2.1. $\mathbf{D}_{n1}$ and $\mathbf{D}_{n2}$

According to Equation (10), the transverse displacement of the *n*th segment is

$$\tilde{Y}_n(\gamma_n)=\gamma_n^{-1}\left[T_{n1}J_2\left(\lambda\sqrt{\gamma_n}\right)+T_{n2}Y_2\left(\lambda\sqrt{\gamma_n}\right)+T_{n3}I_2\left(\lambda\sqrt{\gamma_n}\right)+T_{n4}K_2\left(\lambda\sqrt{\gamma_n}\right)\right] \tag{14}$$

where

$$\gamma_n=\left[(\alpha-1)\tilde{x}_n+1\right],\quad \tilde{x}_n=x_n/L \tag{15}$$

Thus, the continuous conditions at the *n*th damper's location requires that

$$\tilde{Y}_n^{\mathrm{R}}(\gamma_n)=\tilde{Y}_{n+1}^{\mathrm{L}}(\gamma_n) \tag{16}$$

$$\tilde{Y}_n'^{\mathrm{R}}(\gamma_n)=\tilde{Y}_{n+1}'^{\mathrm{L}}(\gamma_n) \tag{17}$$

Considering the force equilibrium conditions at the *n*th damper's location, one has

$$EI(\gamma_n)\frac{\partial^2\tilde{y}_n^{\mathrm{R}}(\gamma_n,t)}{\partial\gamma^2}+C_{dn}\frac{L}{\alpha-1}\frac{\partial^2\tilde{y}_n^{\mathrm{R}}(\gamma_n,t)}{\partial\gamma\partial t}-EI(\gamma_n)\frac{\partial^2\tilde{y}_{n+1}^{\mathrm{L}}(\gamma_n,t)}{\partial\gamma^2}=0 \tag{18}$$

$$\frac{\partial}{\partial\gamma}\left[EI(\gamma_n)\frac{\partial^2\tilde{y}_n^{\mathrm{R}}(\gamma_n,t)}{\partial\gamma^2}\right]=\frac{\partial}{\partial\gamma}\left[EI(\gamma_n)\frac{\partial^2\tilde{y}_{n+1}^{\mathrm{L}}(\gamma_n,t)}{\partial\gamma^2}\right] \tag{19}$$

where C_{dn} is the damping coefficient of the nth damper, the superscript 'R' refers to the right section of the segment, as well as 'L' the left section of the segment.

The substitution of Equation (14) into Equations (16)-(19) leads to

$$\begin{aligned}&T_{n1}J_2\left(\lambda\sqrt{\gamma_n}\right)+T_{n2}Y_2\left(\lambda\sqrt{\gamma_n}\right)\\&+T_{n3}I_2\left(\lambda\sqrt{\gamma_n}\right)+T_{n4}K_2\left(\lambda\sqrt{\gamma_n}\right)\\&-T_{n+1,1}J_2\left(\lambda\sqrt{\gamma_n}\right)-T_{n+1,2}Y_2\left(\lambda\sqrt{\gamma_n}\right)\\&-T_{n+1,3}I_2\left(\lambda\sqrt{\gamma_n}\right)-T_{n+1,4}K_2\left(\lambda\sqrt{\gamma_n}\right)=0\end{aligned} \tag{20a}$$

$$
\begin{aligned}
&T_{n1}J_3\left(\lambda\sqrt{\gamma_n}\right)+T_{n2}Y_3\left(\lambda\sqrt{\gamma_n}\right)\\
&-T_{n3}I_3\left(\lambda\sqrt{\gamma_n}\right)+T_{n4}K_3\left(\lambda\sqrt{\gamma_n}\right)\\
&-T_{n+1,1}J_3\left(\lambda\sqrt{\gamma_n}\right)-T_{n+1,2}Y_3\left(\lambda\sqrt{\gamma_n}\right)\\
&+T_{n+1,3}I_3\left(\lambda\sqrt{\gamma_n}\right)-T_{n+1,4}K_3\left(\lambda\sqrt{\gamma_n}\right)=0
\end{aligned}
\tag{20b}
$$

$$
\begin{aligned}
&T_{n1}\eta_{n1}+T_{n2}\eta_{n2}+T_{n3}\eta_{n3}+T_{n4}\eta_{n4}\\
&-T_{n+1,1}J_4\left(\lambda\sqrt{\gamma_n}\right)-T_{n+1,2}Y_4\left(\lambda\sqrt{\gamma_n}\right)\\
&-T_{n+1,3}I_4\left(\lambda\sqrt{\gamma_n}\right)-T_{n+1,4}K_4\left(\lambda\sqrt{\gamma_n}\right)=0
\end{aligned}
\tag{20c}
$$

$$
\begin{aligned}
&T_{n1}\varsigma_{n1}+T_{n2}\varsigma_{n2}+T_{n3}\varsigma_{n3}+T_{n4}\varsigma_{n4}\\
&-T_{n+1,1}\varsigma_{n1}-T_{n+1,2}\varsigma_{n2}-T_{n+1,3}\varsigma_{n3}-T_{n+1,4}\varsigma_{n4}=0
\end{aligned}
\tag{20d}
$$

where

$$
k_n=\frac{C_n}{\gamma_n^{\frac{7}{2}}}i\sqrt{\tilde{\omega}} \tag{21}
$$

and the non-dimensional damping coefficient takes a form of

$$
C_n=\frac{C_{dn}h_0}{(12\rho E)^{\frac{1}{2}}LI_0} \tag{22}
$$

and

$$
\eta_{n1}=J_4\left(\lambda\sqrt{\gamma_n}\right)-k_nJ_3\left(\lambda\sqrt{\gamma_n}\right) \tag{23a}
$$

$$
\eta_{n2}=Y_4\left(\lambda\sqrt{\gamma_n}\right)-k_nY_3\left(\lambda\sqrt{\gamma_n}\right) \tag{23b}
$$

$$
\eta_{n3}=I_4\left(\lambda\sqrt{\gamma_n}\right)+k_nI_3\left(\lambda\sqrt{\gamma_n}\right) \tag{23c}
$$

$$
\eta_{n4}=K_4\left(\lambda\sqrt{\gamma_n}\right)-k_nK_3\left(\lambda\sqrt{\gamma_n}\right) \tag{23d}
$$

$$
\varsigma_{n1}=8J_4\left(\lambda\sqrt{\gamma_n}\right)-\lambda\sqrt{\gamma_n}J_5\left(\lambda\sqrt{\gamma_n}\right) \tag{24a}
$$

$$
\varsigma_{n2}=8Y_4\left(\lambda\sqrt{\gamma_n}\right)-\lambda\sqrt{\gamma_n}Y_5\left(\lambda\sqrt{\gamma_n}\right) \tag{24b}
$$

$$
\varsigma_{n3}=8I_4\left(\lambda\sqrt{\gamma_n}\right)+\lambda\sqrt{\gamma_n}I_5\left(\lambda\sqrt{\gamma_n}\right) \tag{24c}
$$

$$
\varsigma_{n4}=8K_4\left(\lambda\sqrt{\gamma_n}\right)-\lambda\sqrt{\gamma_n}K_5\left(\lambda\sqrt{\gamma_n}\right) \tag{24d}
$$

Taking advantage of matrix, Equation (20) can be rewritten as

$$
\left[\mathbf{D}_{n1},\mathbf{D}_{n2}\right]\begin{Bmatrix}\mathbf{T}_n\\ \mathbf{T}_{n+1}\end{Bmatrix}=0 \tag{25}
$$

where

$$
\mathbf{D}_{n1}=\begin{bmatrix}
J_2(\lambda\sqrt{\gamma_n}) & Y_2(\lambda\sqrt{\gamma_n}) & I_2(\lambda\sqrt{\gamma_n}) & K_2(\lambda\sqrt{\gamma_n})\\
J_3(\lambda\sqrt{\gamma_n}) & Y_3(\lambda\sqrt{\gamma_n}) & -I_3(\lambda\sqrt{\gamma_n}) & K_3(\lambda\sqrt{\gamma_n})\\
\eta_{n1} & \eta_{n2} & \eta_{n3} & \eta_{n4}\\
\varsigma_{n1} & \varsigma_{n2} & \varsigma_{n3} & \varsigma_{n4}
\end{bmatrix} \tag{26}
$$

and

$$
\mathbf{D}_{n2}=-\begin{bmatrix}
J_2(\lambda\sqrt{\gamma_n}) & Y_2(\lambda\sqrt{\gamma_n}) & I_2(\lambda\sqrt{\gamma_n}) & K_2(\lambda\sqrt{\gamma_n})\\
J_3(\lambda\sqrt{\gamma_n}) & Y_3(\lambda\sqrt{\gamma_n}) & -I_3(\lambda\sqrt{\gamma_n}) & K_3(\lambda\sqrt{\gamma_n})\\
J_4(\lambda\sqrt{\gamma_n}) & Y_4(\lambda\sqrt{\gamma_n}) & I_4(\lambda\sqrt{\gamma_n}) & K_4(\lambda\sqrt{\gamma_n})\\
\varsigma_{n1} & \varsigma_{n2} & \varsigma_{n3} & \varsigma_{n4}
\end{bmatrix} \tag{27}
$$

2.2. $\mathbf{D_L}$ and $\mathbf{D_R}$

Fig. 2.2 illustrates four typically supported beams. The coefficient sub-matrixes DL and DR would be correspondingly obtained by applying the boundary conditions of the ends of these beams. Take a cantilever beam with its left end free and right end clamped as an example. Thus, the boundary conditions are

$$
\tilde{Y}''(1)=0\ ,\ \tilde{Y}'''(1)=0 \tag{28}
$$

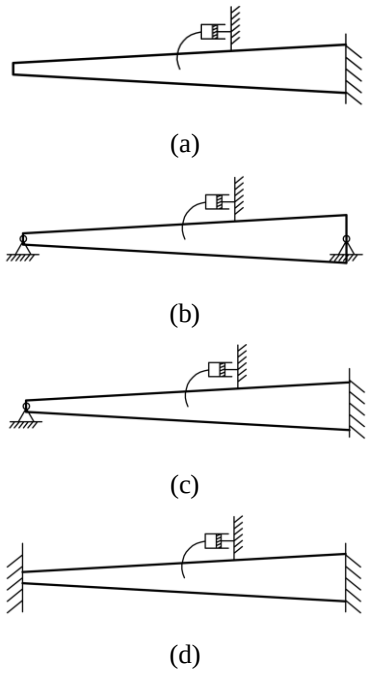

(a) (b) (c) (d)

Figure. 2.2. Beam-damper systems: (a) Cantilever beam. (b) Simply supported beam. (c) Hinged-clamped beam. (d) Clamped-clamped beam.

By substitution of Equation (10) into Equation (28), one obtains

$$T_{11}J_4(\lambda)+T_{12}Y_4(\lambda)+T_{13}I_4(\lambda)+T_{14}K_4(\lambda)=0 \quad (29a)$$

$$T_{11}J_5(\lambda)+T_{12}Y_5(\lambda)-T_{13}I_5(\lambda)+T_{14}K_5(\lambda)=0 \quad (29b)$$

Taking the advantage of matrix, Equation (29) could be rewritten as

$$\mathbf{D}_{\mathrm{L}}\mathbf{T}_1=0 \quad (30)$$

in which

$$\mathbf{D}_{\mathrm{L}}=\begin{bmatrix} J_4(\lambda) & Y_4(\lambda) & I_4(\lambda) & K_4(\lambda) \\ J_5(\lambda) & Y_5(\lambda) & -I_5(\lambda) & K_5(\lambda) \end{bmatrix} \quad (31)$$

At the clamped right end, the boundary conditions are

$$\tilde{Y}(\alpha)=0\ ,\ \ \tilde{Y}'(\alpha)=0 \quad (32)$$

In the same manner, one obtains

$$T_{N+1,1}J_2\left(\lambda\sqrt{\alpha}\right)+T_{N+1,2}Y_2\left(\lambda\sqrt{\alpha}\right)+ T_{N+1,3}I_2\left(\lambda\sqrt{\alpha}\right)+T_{N+1,4}K_2\left(\lambda\sqrt{\alpha}\right)=0 \quad (33a)$$

$$T_{N+1,1}J_3\left(\lambda\sqrt{\alpha}\right)+T_{N+1,2}Y_3\left(\lambda\sqrt{\alpha}\right)- T_{N+1,3}I_3\left(\lambda\sqrt{\alpha}\right)+T_{N+1,4}K_3\left(\lambda\sqrt{\alpha}\right)=0 \quad (33b)$$

and

$$\mathbf{D}_{\mathrm{R}}\mathbf{T}_{N+1}=0 \quad (34)$$

where

$$\mathbf{D}_{\mathrm{R}}=\begin{bmatrix} J_2(\lambda\sqrt{\alpha}) & Y_2(\lambda\sqrt{\alpha}) & I_2(\lambda\sqrt{\alpha}) & K_2(\lambda\sqrt{\alpha}) \\ J_3(\lambda\sqrt{\alpha}) & Y_3(\lambda\sqrt{\alpha}) & -I_3(\lambda\sqrt{\alpha}) & K_3(\lambda\sqrt{\alpha}) \end{bmatrix} \quad (35)$$

Accordingly, all sub-matrixes in coefficient matrix **D** are available, and they would be used to achieve the frequency equation.

For the other beams those having different supports, as shown in Fig. 2.2, the corresponding coefficient sub-matrixes $\mathbf{D}_{\mathrm{L}}$ and $\mathbf{D}_{\mathrm{R}}$ could be addressed by the following Equations (36)-(38) respectively.

For a simply supported beam as shown in Fig. 2.2 (b), one has

$$\mathbf{D}_{\mathrm{L}}=\begin{bmatrix} J_2(\lambda) & Y_2(\lambda) & I_2(\lambda) & K_2(\lambda) \\ J_4(\lambda) & Y_4(\lambda) & I_4(\lambda) & K_4(\lambda) \end{bmatrix} \quad (36a)$$

$$\mathbf{D}_{\mathrm{R}}=\begin{bmatrix} J_2(\lambda\sqrt{\alpha}) & Y_2(\lambda\sqrt{\alpha}) & I_2(\lambda\sqrt{\alpha}) & K_2(\lambda\sqrt{\alpha}) \\ J_4\left(\lambda\sqrt{\alpha}\right) & Y_4\left(\lambda\sqrt{\alpha}\right) & I_4\left(\lambda\sqrt{\alpha}\right) & K_4\left(\lambda\sqrt{\alpha}\right) \end{bmatrix} \quad (36b)$$

For a hinged –clamped beam as shown in Fig. 2.2 (c), one has

$$\mathbf{D}_{\mathrm{L}}=\begin{bmatrix} J_2(\lambda) & Y_2(\lambda) & I_2(\lambda) & K_2(\lambda) \\ J_4(\lambda) & Y_4(\lambda) & I_4(\lambda) & K_4(\lambda) \end{bmatrix} \quad (37a)$$

$$\mathbf{D}_{\mathrm{R}}=\begin{bmatrix} J_2(\lambda\sqrt{\alpha}) & Y_2(\lambda\sqrt{\alpha}) & I_2(\lambda\sqrt{\alpha}) & K_2(\lambda\sqrt{\alpha}) \\ J_3(\lambda\sqrt{\alpha}) & Y_3(\lambda\sqrt{\alpha}) & -I_3(\lambda\sqrt{\alpha}) & K_3(\lambda\sqrt{\alpha}) \end{bmatrix} \quad (37b)$$

For a clamped-clamped beam as shown in Fig. 2.2 (d), one has

$$\mathbf{D}_{\mathrm{L}}=\begin{bmatrix} J_2(\lambda) & Y_2(\lambda) & I_2(\lambda) & K_2(\lambda) \\ J_3(\lambda) & Y_3(\lambda) & -I_3(\lambda) & K_3(\lambda) \end{bmatrix} \quad (38a)$$

$$\mathbf{D}_{\mathrm{R}}=\begin{bmatrix} J_2(\lambda\sqrt{\alpha}) & Y_2(\lambda\sqrt{\alpha}) & I_2(\lambda\sqrt{\alpha}) & K_2(\lambda\sqrt{\alpha}) \\ J_3(\lambda\sqrt{\alpha}) & Y_3(\lambda\sqrt{\alpha}) & -I_3(\lambda\sqrt{\alpha}) & K_3(\lambda\sqrt{\alpha}) \end{bmatrix} \quad (38b)$$

3. Solving Characteristic Equation

The nontrivial solution of Equation (11) requires that the determinant of the matrix **D** is zero, i.e.

$$\det\mathbf{D}=0 \quad (39)$$

Equation (39) is the characteristic equation that governs the system's complex natural frequencies.

The presence of the rotational dampers renders the characteristic equation complex valued. And the explicit form of the solution of the Equation (39) is hard to be obtained due to the presence of the Bessel function. Thus, numerical method is introduced herein to achieve the numerical solutions of Equation (39).

The left term of Equation (39) is regarded as a function of $\tilde{\omega}$, i.e.

$$f(\tilde{\omega})=\det\mathbf{D} \quad (40)$$

Accordingly, the zeros of function f would be the solutions of Equation (39).

Then, we define an objective function χ in a form of

$$\chi = \left[\mathrm{Im}(f(\tilde{\omega}))\right]^2 + \left[\mathrm{Re}(f(\tilde{\omega}))\right]^2 \quad (41)$$

By giving an acceptable error ε and appropriate initial values of $\tilde{\omega}$ in advance, minimizing χ would lead to approximate zeros of the function $f(\tilde{\omega})$. Note that the angular frequency $\tilde{\omega}$ is in complex domain. Accordingly, there are two variables, i.e. the real and imaginary parts of the $\tilde{\omega}$, in the defined function χ. And, the optimizing methodology employed should be suitable for multi-variable searching.

Note that there exist many complex valued zeros of $f(\tilde{\omega})$. The main difficulty in searching the zeros of χ is to determinate the initial values. Tracing technique is used to determine the initial value. Consider an original system and a new system. The damping caused by the dampers of the new system is slightly greater than the original system. Note that there exists a sufficiently small difference of damping which let the optimizing method could find the zeros of χ of the new system by letting the initial values are equal to those of the original system. Whereby, the solution of the damped system could be achieved by increasing the damping in steps, if the damping difference between the two adjacent steps is small enough.

Actually, the natural frequencies appear in complex conjugate pairs. In this paper, we merely consider the natural frequencies having a form of

$$i\tilde{\omega} = -\xi\omega_0 + \sqrt{1-\xi^2}\,\omega_0 i \quad (42)$$

where ξ is the damping ratio, and ω_0 is the pseudo-undamped natural frequency.

Then Gaussian elimination can be used to determine the unknown T_{ij}, by substitution of the value of $\tilde{\omega}_m\,(m=1,2,\cdots,5)$ into Equation (11). If the non-dimensional natural frequencies $\tilde{\omega}_m$ and the constants $\mathbf{T}_n\,(n=1,2,\cdots,N+1)$ are available, one may then attain the mode shapes of the constrained beam.

4. Numerical Results and Discussions

4.1. Comparing with FEA Results

To ensure the reliability of the presented algorithm, Finite Elements Analysis (FEA) is employed for comparison. The cubic shape functions of the beam element are

$$W_1 = 1 - 3(\frac{\bar{x}}{L_n})^2 + 2(\frac{\bar{x}}{L_n})^3 \quad (43a)$$

$$W_2 = \bar{x} - 2L(\frac{\bar{x}}{L_n})^2 + L(\frac{\bar{x}}{L_n})^3 \quad (43b)$$

$$W_3 = 3(\frac{\bar{x}}{L_n})^2 - 2(\frac{\bar{x}}{L_n})^3 \quad (43c)$$

$$W_4 = -L(\frac{\bar{x}}{L_n})^2 + L(\frac{\bar{x}}{L_n})^3 \quad (43d)$$

where $\bar{x}$ is the abscissa in local coordinate system, and L_n is the length of the element. Thus, the global mass, damping and stiffness matrixes, designated as **M**, **C** and **K** respectively, could be obtained by using (43) and the theory of the FEA. Accordingly, the motion equation of the beam-damper system could be written in a discrete form of

$$\mathbf{M}\ddot{\mathbf{U}} + \mathbf{C}\dot{\mathbf{U}} + \mathbf{K}\mathbf{U} = 0 \quad (44)$$

in which **U** is the vector of the nodal transverse displacements.

Equation (44) can be rewritten in state-space as

$$\dot{\mathbf{Z}} = \mathbf{A}\mathbf{Z} \quad (45)$$

where the system matrix A are

$$\mathbf{A} = \begin{bmatrix} \mathbf{0} & \mathbf{I} \\ -\mathbf{M}^{-1}\mathbf{K} & -\mathbf{M}^{-1}\mathbf{C} \end{bmatrix} \quad (46)$$

in which **0** is a null matrix, **I** is an identity matrix. Thus, the complex valued eigenvalues of the system matrix **A** would lead to the pairs of conjugated natural frequencies of the whole system. And, the natural frequencies those having the form of Equation (42a) are selected for comparison.

Two examples are considered herein for the verification of the validity of the present methodology. Example I is a hinged-clamped (h-c) tapered beam whose taper ratios $\alpha = \beta = 2$. Two rotational dampers are installed and located at $\tilde{x}_1 = 0.3$ and $\tilde{x}_2 = 0.6$ respectively. The damping of the former (the first damper) is fixed, i.e. C_1=1. Example II is a free-clamped (f-c) tapered beam attached with one rotational damper whose location is $\tilde{x}_1 = 0.5$, and the taper ratios of the beam are $\alpha = \beta = 2$. In Example I, by altering the damping of the damper at $\tilde{x}_2 = 0.6$, the root loci of the first five natural frequencies are illustrated in Fig. 4.1 (a). In Example II, by altering the damping of the

damper, the root loci of the first five natural frequencies are illustrated in Fig. 4.1 (b). The arrows in Fig. 4.1 denote the increasing of the damping, and the increment is 0.01. In similar fashion, the curves of the damping ratios versus the damping of the altered damper were shown in Fig. 4.2.

For the sake of comparison, the FEA results are correspondingly plotted in both Fig. 4.1and Fig. 4.2. Good agreement is observed, which confirms the validity of the present method.

Fig. 4.3 shows the first five normalized mode shapes of two examples. The $\tilde{Y}_0$ in the figure is the value whose modulus is the maximum value of the whole mode, that is to say $\left|\tilde{Y}_0\right| = \max\left|\tilde{Y}(\tilde{x})\right|$. In Example I, the value of damping of the second damper is 1. In Example II, the damping of the damper is 0.05. The comparison of the results obtained by FEA and the present methodology indicates a good agreement, which verified the validity of the method.

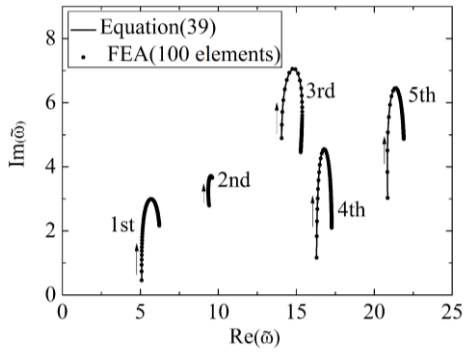

(a)

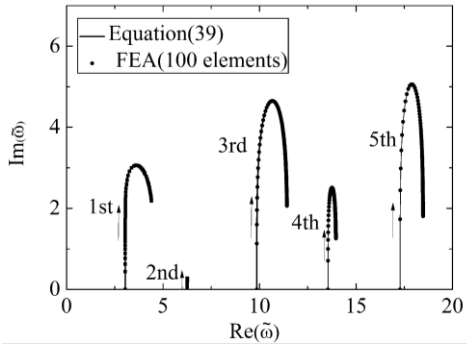

(b)

Figure. 4.1. The root loci of the first five natural frequencies for the two examples: (a) Example I. (b) Example II.

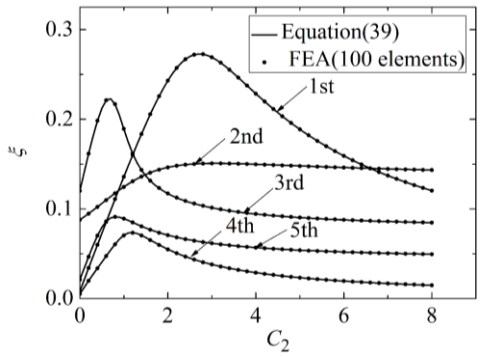

(a)

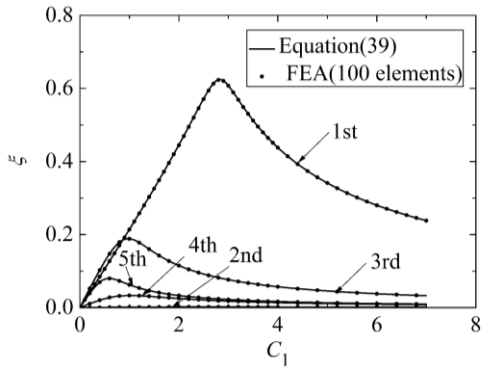

(b)

Figure. 4.2. The lowest five damping ratios versus the damping of the altered damper for the two examples: (a) Example I. (b) Example II.

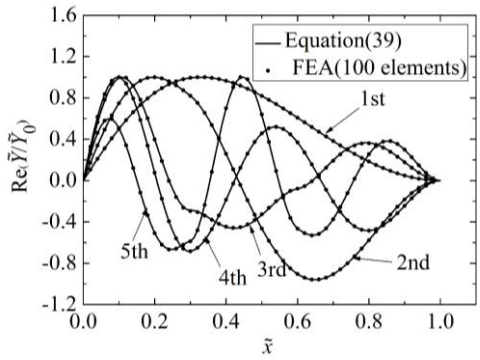

(a)

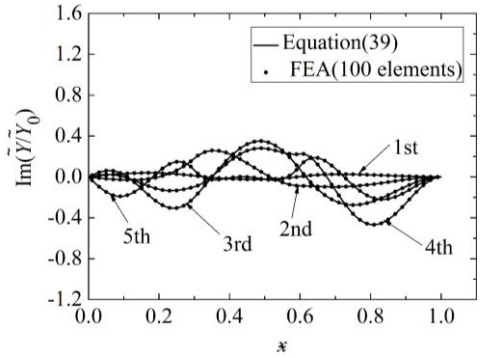

(b)

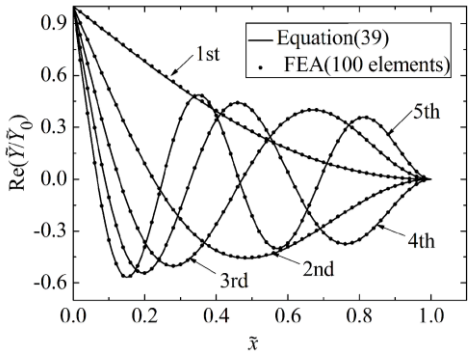

(c)

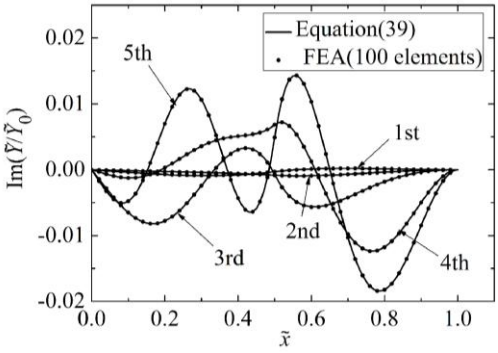

(d)

Figure 4.3. The first five normalized mode shapes of two examples: (a) Real part in Example I. (b) Imaginary part in Example I. (c) Real part in Example II. (d) Imaginary part in Example II.

4.2. System Damping Ratio

It could be observed from Fig. 4.1 that there exists a maximum modal damping ratio $\xi_{\max}$. Also, for different modes, the maximum damping ratios and the corresponding damping coefficients are different. To investigate the relationship between the maximum damping ratio $\xi_{\max}$ and the taper ratio α, eight types of ratio were considered herein.

Fig. 4.4 illustrates the curves of the maximum damping ratio versus the damper's position. It is observed that the value of $\xi_{\max}$ is varied with the position and taper ratio. It is found that the curves have peak values, and the number of the peak values of a curve is equal to its corresponding mode order whatever the taper ratio is. It is illustrated that the position of the peak value is slightly effected by the taper ratio, but significantly related to the mode order. The increasing of the taper ratio would reduce the peak values. It is found that the reduction would be relative small, if the taper ratio exceeds 7. The similar phenomena would be observed, according the curves those belong to the third, fourth and fifth modes and are not illustrated herein.

The non-dimensional damping corresponding to the maximum damping ratio is designated as optimal damping coefficient C_{opt}. It is varied with the damper's position, and depicted in Fig. 4.5. It is found that the optimal damping coefficient of the damper would increase rapidly, if the damper is near the fixed end of the beam. This leads to a suggestion of the position of the damper that the damper's position is less than 0.75, for the purpose of economy. The comparison of the curves of different taper ratios indicates that the optimal damping of the damper should increase quickly with the increment of the taper ratio.

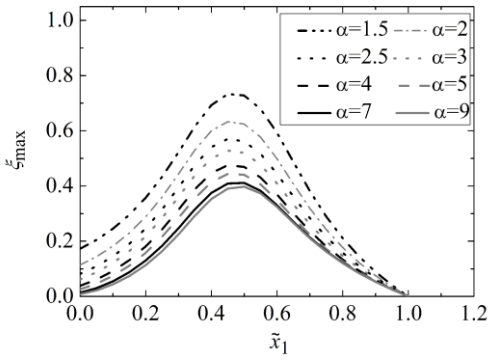

(a)

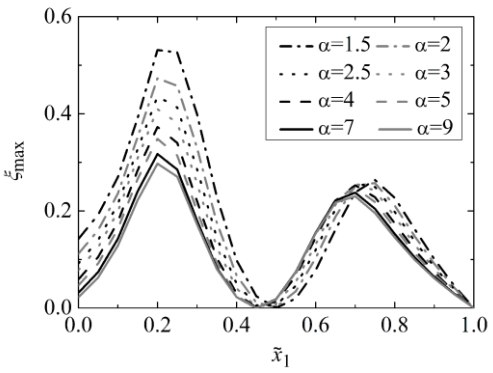

(b)

Figure. 4.4. Maximum damping ratio: (a) First mode. (b) Second mode.

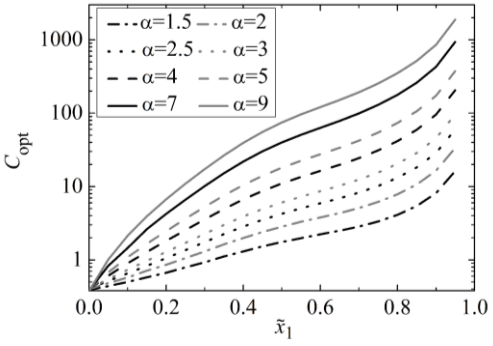

(a)

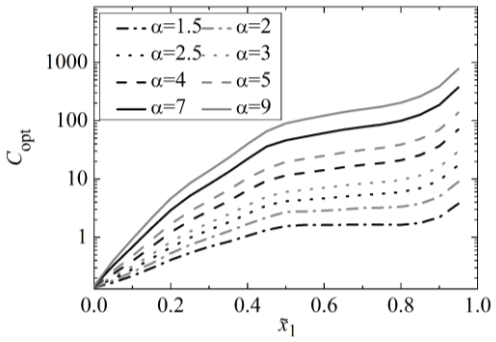

(b)

Figure. 4.5. Optimal damping coefficient: (a) First model. (b) Second model.

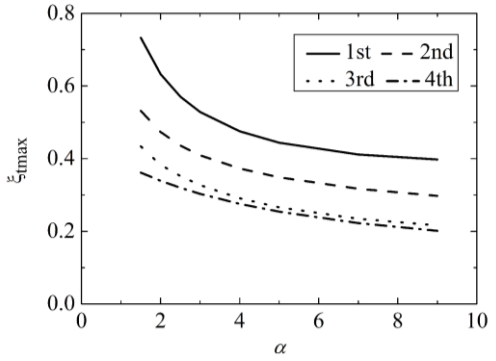

Figure. 4.6. Total maximum damping ratios for the first four modes.

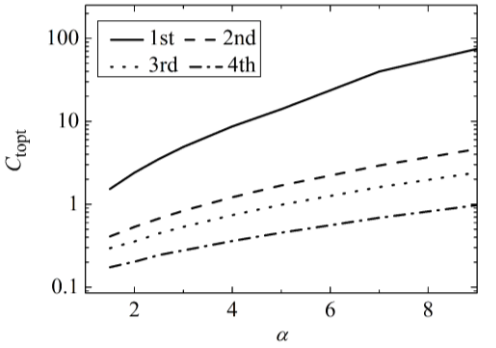

Figure. 4.7. Total optimal damping coefficients for the first four modes.

For a given mode, the maximum of the peak values of a curve as depicted in Fig. 4.4 is designated as the total maximum damping ratio of this mode, and denoted as ξ_{tmax}. Accordingly, the damper is located at the optimal position. The value of it is merely related to the taper ratio and mode order. Fig. 4.6 shows the curves of ξ_{tmax} versus the taper ratio. It is found that the total maximum damping ratio decrease with increasing the taper ratio. Also, the higher the order of the mode is, the smaller the total maximum damping ratio is.

Total optimal damping coefficient is denoted as C_{topt}, and corresponds to the total maximum damping ratio. Fig. 4.7 shows the varying of it with the taper ratio. It is found that the total optimal damping coefficient increase with increasing the taper ratio. The smaller it would be, the higher mode order it belongs to. For the second mode or the modes of higher order, the difference between the total optimal damping coefficients is relatively small.

5. Conclusions

Free vibration of a tapered beam with multiple rotational dampers is examined. The Bessel functions are employed to address the exact free vibration of a double tapered beam without dampers. The continuous conditions at where the rotational dampers are installed are presented, so that NAM could be applied to achieve the exact solution of the system. The characteristic equation, which is described in complex domain, of the whole system is derived, and is suitable for different boundary conditions.

To finding the solution of the characteristic equation, the left of it is regarded as a function of the natural frequency. A method to determine the zeros of this function is therefore proposed. By minimizing a constructed objective function, the proposed method is capable of attaining the real and imaginary part of the zeros simultaneously. The comparison of the results obtained by FEA and the present method indicates a good agreement, which confirms the validity of the present method.

The analysis on a cantilever beam with one rotational damper is conducted. It is found that there exists a maximum damping ratio and corresponding optimal damping. The effectiveness of the rotational damper is observed. The maximum damping ratio would decreases and corresponding optimal damping would increases, if the taper ratio increases. For the first four modes, a lower mode order leads to a larger optimal damping and a higher maximum damping ratio. The similar phenomena would be found, if one surveys the total maximum damping ratio and the total optimal damping coefficient those determined by installing the damper at the optimal location and tuning the damper to the optimal.

Acknowledgements

The authors acknowledge the financial support offered by Ministry of Transport of the People's Republic of China, project No. 2011318223170. The author is grateful to the anonymous referee for a careful checking of the details and for helpful comments that improved this paper.

References

[1] N.M. Auciello, *Transverse vibrations of a linearly tapered cantilever beam with tip mass of rotatory inertia and eccentricity*, *Journal of Sound and Vibration*, 194, 25 -34 (1996).

[2] M.A. De Rosa and N.M. Auciello, *Free Vibrations of Tapered Beams with Flexible Ends*, *Computers and Structures*, 60, 197-202 (1996).

[3] R.P. Goel, *Transverse Vibrations of Tapered Beams*, *Journal of Sound and Vibration*, 47, 1-7 (1976)

[4] H.H. Mabie, C.B. Rogers, *Transverse vibrations of tapered cantilever beams with end loads*, *Journal of the Acoustical Society of America*, 36, 463-469 (1964).

[5] H.H. Mabie, C.B. Rogers, *Transverse vibrations of tapered cantilever beams with end support*, *Journal of the Acoustical Society of America*, 44, 1739-1741 (1968).

[6] H.H. Mabie, C.B. Rogers, *Transverse vibrations of double-tapered cantilever beams*, *Journal of the Acoustical Society of America*, 51, 1771-1774 (1972).

[7] H.H. Mabie, C.B. *Rogers, Transverse vibrations of double-tapered cantilever beams with end support and with end mass*, *Journal of the Acoustical Society of America*, 55, 986-991 (1974).

[8] S.I. Alvarez, G.M. Ficcadenti De Iglesias and P.A.A. Laura, *Vibrations of an elastically restrained, non-uniform beam with translational and rotational springs, and with a tip mass*, *Journal of Sound and Vibration*, 120, 465-471 (1991).

[9] D.W. Chen and J.S. Wu, *The exact solutions for the natural frequencies and mode shapes of non-uniform beams with multiple spring-mass systems*, *Journal of Sound and Vibration*, 255, 299-322 (2002).

[10] W.L. Craver and P. Jampala, *Transverse vibrations of a linearly tapered cantilever beam with constraining springs*, *Journal of Sound and Vibration*, 166, 521-529 (1993).

[11] Q.S. Li, *Free vibration analysis of non-uniform beams with an arbitrary number of cracks and concentrated masses*, *Journal of Sound and Vibration*, 252, 509-525 (2002).

[12] H. Qiao, Q.S. Li and G.Q. Li, Vibratory characteristics of flexural non-uniform Euler-Bernoulli beams carrying an arbitrary number of spring-mass systems, International Journal of Mechanical Sciences, 44, 725-743 (2002).

[13] G.V. Sankaran, K.K. Raju and G.V. Rao, *Vibration frequencies of a tapered beam with one end spring-hinged and carrying a mass at the other free end*, *Journal of Applied Mechanics-Transactions of the ASME*, 42, 740-741 (1975).

[14] K.Y. Yang, *The natural frequencies of a non-uniform beam with a tip mass and with translational and rotational springs*, *Journal of Sound and Vibration*, 137, 339-341 (1990).

[15] G. Oliveto, A. Santini and E. Tripodi, *Complex modal analysis of a flexural vibrating beam with viscous end conditions*, *Journal of Sound and Vibration*, 200, 327-345 (1997).

[16] S. Krenk, *Complex modes and frequencies in damped structural vibrations*, *Journal of Sound and Vibration*, 270, 981-996 (2004).

[17] K. Engelen, H. Ramon and W. Saeys, W. Franssens and J. Anthonis, *Positioning and tuning of viscous damper on flexible structure*, *Journal of Sound and Vibration*, 304, 845-862 (2007).

[18] N. Impollonia, G. Ricciardi and F.K. Saitta, *Dynamic behavior of stay cables with rotational dampers*, *Journal of Engineering Mechanics*, 136, 697-709 (2010).

[19] Y. Chen, D.M. McFarland, Z. Wang, B.F. Spencer and L.A. Bergman, *Analysis of tall buildings with damped outriggers*, *Journal of Structural Engineering*, 136, 1435-1443 (2010)

Yong Chen is an associate professor employed by Zhejiang University, Hangzhou (China). He obtained his PHD from Zhejiang University (China). His main research field including structural engineering, health monitoring, damage detection, wind engineering, and vibration control. He has over 70 correlated journal papers are published (in Chinese or in English).

Pan Liu is a researcher in structural engineering and is employed by Hangzhou Architectural Design and Research Institute, Hangzhou (China). She obtained her MS from Zhejiang University (China). Her main research work is on the continuous system attached with discrete subsystem.